# Temperature-insensitive source for entangled time-frequency quantum photonic states

Daniel Gauthier, Andrew Rockovich
Dept. of Physics, The Ohio State University, 191 W Woodruff Ave., Columbus, OH 43210, USA

## ABSTRACT

We describe a method for reducing the temperature sensitivity for spontaneous parametric down conversion (SPDC) suitable for generating entangled time-frequency quantum photonic states in the telecommunication band at a wavelength of 1550 nm. We present specific design examples using periodically-poled $LiNbO_3$ waveguides, which are commercially available and have a high second-order nonlinear coefficient that improves the overall device efficiency. One method uses two distinct poling regions, each with a poling period selected for phase-matching at different temperatures. The temperature bandwidth is increased from ~5 °C to ~17 °C using this approach, while only reducing the overall efficiency of the process by a factor of 4. The bandwidth is large enough so that controlling the overall temperature of the nonlinear crystal is likely not needed in a laboratory environment or can be achieved using a low size, weight, and power temperature controller design for field-deployed sources. To improve the stability of the design, we propose using a differential heating method where only the difference in the temperature is stabilized. The differential temperature stabilization method requires a smaller, lighter weight heater and lower power than other approaches, thus greatly simplifying the overall design. Additionally, we show that the system is less sensitive to fluctuations in the pump laser's wavelength for the two-region approach. Finally, we generalize the design to multiple poling regions.

**Keywords:** Spontaneous parametric down conversion, SPDC, time-frequency entanglement, photonic entanglement, quantum communication, quantum optics, quantum information science

## 1. INTRODUCTION

A key resource for quantum communication technologies is a source of entangled photon pairs. One of the most widely used means of generating entangled photons is through the process of spontaneous parametric down conversion (SPDC), whereby a birefringent nonlinear crystal is pumped by a laser beam at a wavelength of $\lambda_{pump}$ and a pair of photons are generated at the signal ($\lambda_{signal}$) and idler ($\lambda_{idler}$) wavelengths. Energy must be conserved in the interaction, thus requiring that $1/\lambda_{pump} = 1/\lambda_{signal} + 1/\lambda_{idler}$.

Waveguide SPDC sources are of great current interest because they confine both the pump and generated pairs, thereby greatly increasing the overall device efficiency and lowering the required pump power. Designing the waveguide is substantially simplified if all waves have the same state of polarization. This polarization configuration lends itself to time-frequency entangled states [1], where the conjugate variables are the time-of-arrival and frequency (energy) of the photons. Here, we focus on methods for generating these states that are more robust to changes in the device temperature.

For efficient SPDC generation, the interaction must also conserve momentum of the photons. This is known as phase-matching. Phase-matching can be achieved by adjusting the direction of propagation of the pump, signal, and idler waves with respect to the crystalline axes (so-called angle tuning). Another approach is to take advantage of the temperature dependence of the index of refraction of the material (temperature tuning). Depending on the wavelengths of the pump, signal, and idler waves, it is not always possible to achieve phase-matching. In some of these cases, it is possible to periodically invert the direction of the crystal axis to achieve what is known as phase-matching by periodic poling [2]. This technique allows access to high nonlinearity in some materials (such as lithium niobate) that would otherwise be unattainable.

For essentially all approaches to phase-matching, the temperature must be tightly controlled to maintain phase-matching. This is due to both changes in poling period (thermal expansion/contraction) as well as changes in the indices of refraction, both shown in Fig. 1 for $LiNbO_3$ and degenerate SPDC producing pairs at 1550 nm. The typical

Advanced Photon Counting Techniques XVIII, edited by Mark A. Itzler, Joshua C. Bienfang, K. Alex McIntosh, Proc. of SPIE Vol. 13025, 1302509 · © 2024 SPIE
0277-786X · doi: 10.1117/12.3017807

temperature stabilization method is to place the nonlinear crystal in a large oven that creates a uniform and controlled temperature over the entire crystal length. Compact designs are possible by directly depositing heating elements on one side of the crystal [2], although the range in achievable temperatures may be limited in this method because large thermal gradients will crack the crystal. These methods both increase the size, weight, and power (SWaP) of the overall photonic entanglement source. This is problematic for applications involving drones, satellites, and any other SWaP-sensitive environment. In environments typical of these applications (space, varying altitudes, etc.), temperatures fluctuate greatly, making temperature insensitivity even more important.

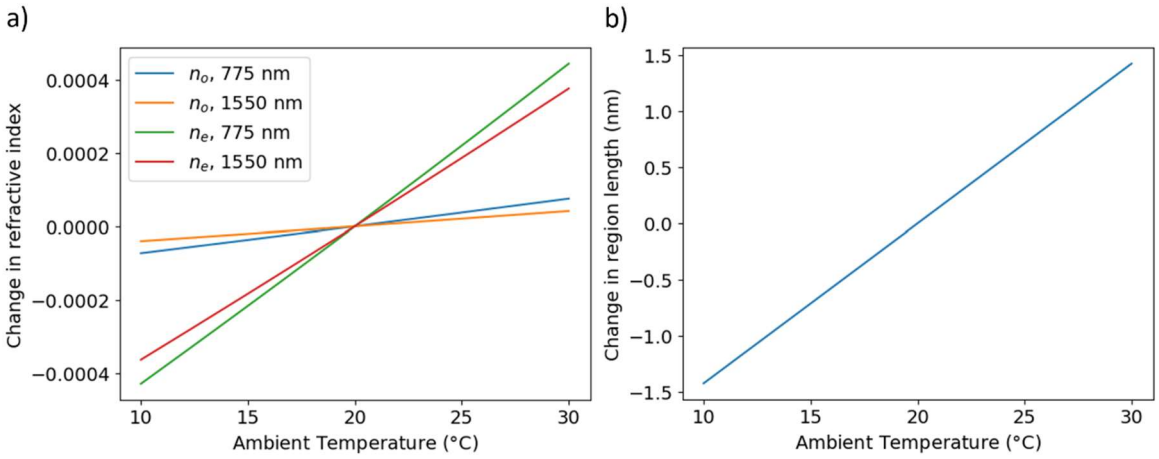


Figure 1. a) The deviation of each index of refraction for $LiNbO_3$ from its value at an ambient temperature of 20 °C. The extraordinary index of refraction is more sensitive to changes in temperature. b) The change in region thickness compared to its phase-matched value at 20 °C (18.990 μm). The plots are generated using the Sellmeier equation with coefficients given in Ref. [6] and the thermal expansion perpendicular to the crystal axis from Ref. [7].

A design for improving the temperature bandwidth (reducing the temperature sensitivity) of SPDC has not been presented in the literature to the best of our knowledge, although it is known that different polarization configurations of the waves have different temperature bandwidths [3] and that methods for increasing the spectral bandwidth of the device improves the temperature bandwidth [4,5]. We are not aware of a purposeful design to increase the temperature bandwidth, which is presented here.

Our innovation is to alter a traditional periodically-poled waveguide to instead include two or more regions of different poling periods ($\Lambda$) chosen for achieving phase-matching at different temperatures, which broadens the temperature bandwidth. The usual one-region design is illustrated in Fig. 2a) and a two-region design is shown in Fig. 2b). The underlying principle of our design relies on a trade-off between phase matching at more temperatures, shortening the interaction length where a certain wavelength is down-converted most efficiently, and making combinations of the spectra from each different poling region coherent. This is discussed further in Section 4, where we deal with incoherences due to manufacturing errors.

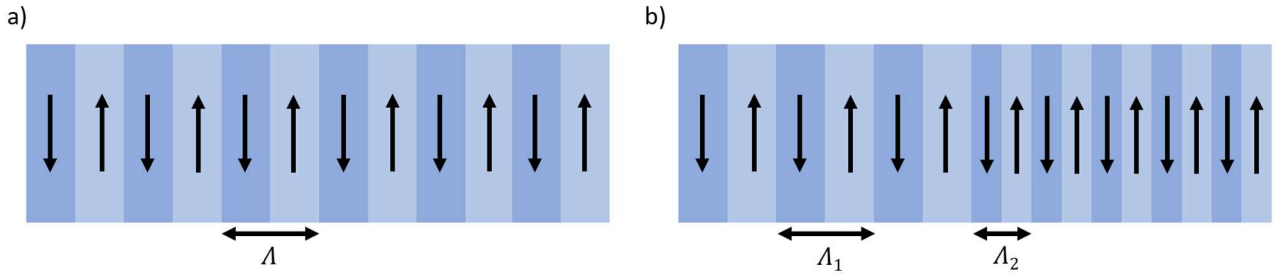


Figure 2. a) The typical design of periodically-poled waveguides, with one poling period, and b) our innovation, where we introduce a second region with a different poling period. The regions are not to scale, the large difference in poling period is for illustrative purposes.

The paper is organized as follow. In Section 2, we lay the groundwork of our simulations and discuss similar work that has been done using a variation of poling period across a waveguide. Section 3 illustrates the efficiency advantage that two-region waveguides have over a range of ambient temperatures. We discuss the correction of manufacturing error using a differential heating design in Section 4. In Section 5, we discuss how the relative efficiency vs. ambient temperature curve changes for pump wavelength detuning, and its implications for the additional efficacy of the two-region waveguide approach for full system temperature insensitivity. In Section 6, we look at the extension of this technique to additional poling periods with a few different techniques for altering them across the waveguide. Lastly, we discuss the trade-off between the magnitude of nonlinearity and temperature bandwidth for different phase-matching configurations, specifically for $LiNbO_3$.

## 2. METHODS

We consider the case for SPDC pumped at $\lambda_{pump}$ = 775 nm and producing degenerate pairs at 1550 nm in a lithium niobate waveguide. We hold these wavelengths fixed, adjust the temperature, and calculate the normalized efficiency given by $\text{sinc}^2(\Delta k\, L)$, where the phase mismatch is $\Delta k = 2\pi[(n_{pump} - (n_{signal}\text{-}n_{idler})/2)/\lambda_{pump}\text{-}1/(mL)]$, $L$ is the crystal length assumed to be 2 cm for the simulations below, $n_{pump}$, $n_{signal}$, and $n_{idler}$ are the indices of refraction at the pump, signal, and idler wavelengths, respectively, $m$ is the order of the interaction, and $\Lambda$ is the poling period. We consider the temperature-dependent refractive index [6] and the thermal expansion of the grating using a thermal expansion coefficient of $7.5\times10^{-6}$ along a direction perpendicular to the crystalline "c" axis [7], that is, along the direction of propagation of the light in the waveguide. The highest efficiency for SPDC occurs when $\Delta k = 0$, known as the condition for perfect phase-matching.

One key concept of our design is to adjust the poling period along the length of the crystal so that different regions are phase-matched at different temperatures. Thus, there is always one region that will contribute to the SPDC process at some temperature. The downside of this approach is the effective length of the interaction region is less than the $L$, thereby reducing the efficiency. For future reference, the efficiency scales as $L^2$ for an ideal SPDC interaction. Furthermore, the SPDC fields must add constructively between the two regions, requiring precise control over the relative poling periods between the regions.

The idea of adjusting the poling period is well known in the literature for increasing the *spectral* bandwidth of the SPDC interaction (see Ref. [8] for a recent example). Methods for increasing the spectral bandwidth include using discrete steps in the poling period along the crystal or a continuous linearly increasing variation (chirp) in the poling period, apodization to reduce ripples in the spectral curve, etc.

We are not aware of anyone that has considered these methods for improving the *temperature* bandwidth of the SPDC process. Any of these methods described above for increasing the *spectral* bandwidth can be adapted to increasing the temperature bandwidth. Initially, we focus on the case of using only two regions with distinct poling periods (step change) and later generalize to more complicated configurations.

## 3. RESULTS

We predict the phase-mismatch as a function of temperature for the Type 0 eee phase-matching configuration (pumping with an extraordinary polarized wave or e-wave, generating two e-waves), which has the highest nonlinearity and hence the highest SPDC efficiency for a given pump power. We consider two cases: 1) the entire crystal length has a single poling period that phase-matches the interaction at temperature $T_1$; and 2) the first half of the crystal has the same poling period as the first case and the second half has a poling period that phase-matches the interaction at temperature $T_2 > T_1$. We optimized the value of $T_2$ by re-running the simulation for different values of $T_2$ and selecting the one that has the most uniform response over the temperature range. Other variations are possible, such as having the first region at a different temperature or having the second region cooler than the first region.

Figure 3 shows the phase-matching curve for the two cases using $T_1$ = 20.0 °C (poling period of 18.990 μm when the temperature is 20.0 °C) and $T_2$ = 30.8 °C (poling period of 18.956 μm when the temperature is 30.8 °C). The first case using a single poling period (blue line) has its efficiency peaked at 20.0 °C as expected and a temperature bandwidth (full width at half maximum of the efficiency curve) of ~5 °C.

For the case of two regions (orange line), there are substantial interactions between the efficiency curves for each region, somewhat "pulling" their peak efficiency away from the phase-matching temperature in each region and creating a peak in efficiency about halfway between the two regions that arises from constructive interference between the generated fields in each region. Given that each region is half the crystal length, we expect that the efficiency should be 1/4 of the efficiency of a single region that spans the full crystal length (horizontal red line) if the phase-matching peaks are well separated so there is no interaction of the field generated in the first and second regions. We see that the efficiency goes somewhat above and below this line. Importantly, the temperature bandwidth has expanded to ~17 °C, which over three times the nominal bandwidth of a single region.

The ripples in the efficiency curve can be reduced by using more step regions, using a continuous linear chirp in the poling period, apodizing the grating, etc. However, these approaches come at an increased manufacturing cost but may be worthwhile in some designs where a flat efficiency curve is an important metric. We discuss these points more in Section 6. Another approach is to adjust the pump laser power as the temperature changes, thus reducing the variation in down-converted photon pair production of the overall system.

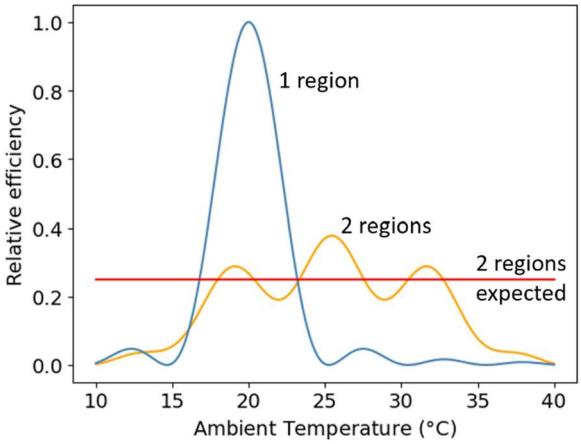


Figure 3. Temperature bandwidth for one and two regions of different poling period in periodically-poled lithium niobate.

## 4. COMPENSATING A MANUFACTURING ERROR USING A DIFFERENTIAL TEMPERATURE

The shape of the efficiency curve is sensitive to small errors in the relative poling period between the two regions because there is interference from the generated SPDC fields in the two regions. Here, we describe a second key innovation to compensate for such errors by making a small adjustment to the temperature difference $\Delta T$ between the regions. This technique exploits a combination of the thermal expansion of the crystal along the direction the light propagates alongside the temperature dependence of the refractive indices.

Figure 4a) shows the efficiency curve for the two-region case when the poling period in the second region is 18.950 mm when the temperature is 30.8 °C. This is a 6.3 nm error in the poling period. The efficiency curve is clearly distorted in comparison to the ideal case shown in Fig. 2 when the temperature is uniform along the crystal. This is a case of incoherent addition of the efficiency curves for the two regions and is an important example of the sensitivity of their interaction with one another. Figure 4b) shows the efficiency curve when $\Delta T$ = 1.9 °C, showing that the ideal efficiency curve is restored.

This result is important from a practical perspective. The overall temperature of the crystal does not need to be controlled, but only the temperature difference of the two regions. Furthermore, $\Delta T$ is small, which will only require a small, lightweight, and low power temperature controller to maintain a relatively flat efficiency curve over a wide overall temperature range.

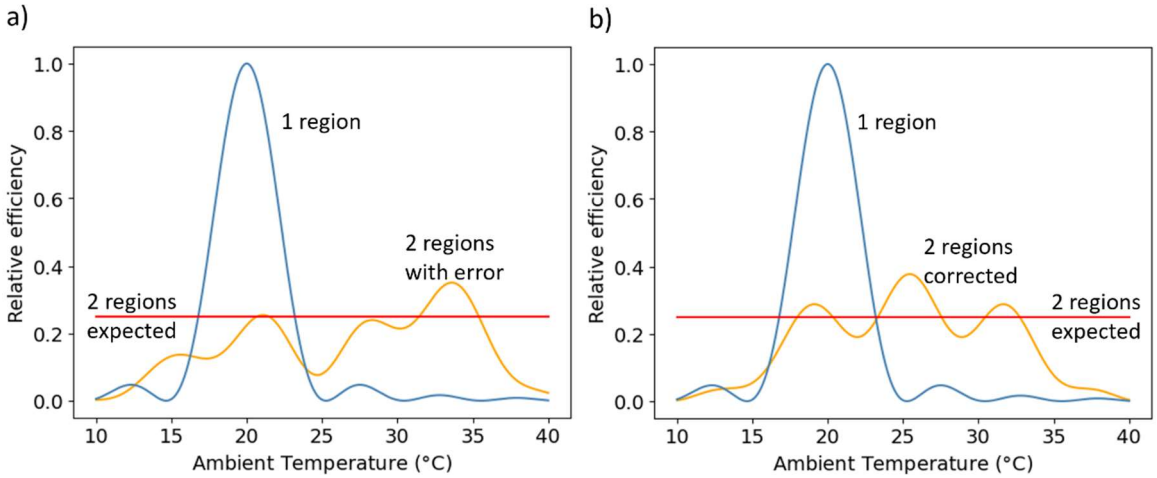


Figure 4. Compensating a manufacturing error using a differential temperature adjustment.

## 5. SENSITIVITY TO PUMP WAVELENGTH DETUNING

Lasers typically have a finite spectral width and a change in wavelength with temperature due to temperature dependent changes in the lasing medium, thermal expansion/contraction of the resonator cavity, or both. Therefore, reducing the periodically-poled waveguide efficiency's sensitivity to changes in the pump laser's wavelength and reducing the temperature sensitivity of the crystal for efficient SPDC are of similar interest. We focus on the former here.

As a result of the pump wavelength changing, the degenerate pairs produced will change wavelength as well to maintain $\lambda_{signal} = \lambda_{idler} = 2\lambda_{pump}$ in accordance with energy conservation. We simulate the effects of changing the pump laser's wavelength on the shape of the relative efficiency curve over ambient temperature. The results are shown in Fig. 5 and 6, where the pump wavelength detuning is $\Delta\lambda_p = \lambda_{pump}$ - 775 nm. It is evident that the two-region approach is less sensitive to changes in pump wavelength compared to the one-region design because the efficiency curve is broader for the two-region design.

It should be noted that a higher temperature will result in the laser producing a longer wavelength, so the shifts in the efficiency curves in Fig. 5 may be less detrimental than they currently appear. To achieve an SPDC system with a one-region waveguide that has the full 5 °C temperature bandwidth (in the one-region case) or more, the system would have to be designed such that the laser spectrum and the waveguide's efficiency have compatible temperature responses. The efficiency curve in Fig. 5b) shows that the two-region case can benefit similarly from considering how the crystal's efficiency and the laser spectrum both shift with ambient temperature. Importantly, the efficiency curve is hardly deformed with changes in pump wavelength, resulting in a much greater overlap in the efficiency curves over temperature for detuned pump wavelengths.

This result shows that the two-region approach is doubly robust to temperature fluctuations – not only is the relative efficiency of SPDC in the crystal less temperature sensitive, but also the temperature-dependent effects from the pump laser are mitigated. Figure 6 illustrates this same idea over a range of pump wavelength detunings, again keeping the down-converted photons degenerate ($\lambda_{signal} = \lambda_{idler} = 2\lambda_{pump}$). Unsurprisingly, the efficiency curves over pump wavelength detuning resemble those over ambient temperature. Crystal temperature and pump wavelength both determine how well the waveguide phase-matches degenerate SPDC interactions, and therefore they have a similar impact on SPDC efficiency.

A typical spectral tuning rate over temperature for semiconductor lasers in the visible wavelength range is about 0.2-0.3 nm/°C. In Fig. 6, this corresponds to a full width at half maximum pump wavelength detuning bandwidth of approximately 1-2 °C and about 3-5 °C for one- and two-region waveguides, respectively. There are designs that mitigate this temperature sensitivity at the source, such as incorporating a Bragg grating, as is done in a distributed-feedback (DFB) laser. These methods can lower temperature tuning coefficient of the laser by about an order-of-

magnitude, which makes the pump laser's temperature bandwidth wider than that of the crystal's efficiency curve for both the one- and two-region waveguides.

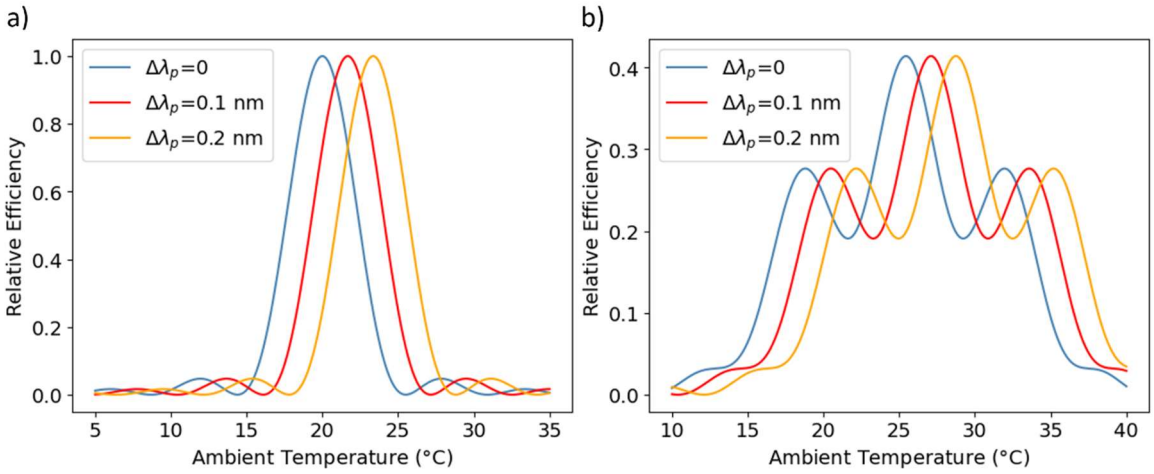


Figure 5. The effect of pump wavelength detuning $\Delta\lambda_p$ on the shape of the relative efficiency curve over the crystal's temperature for both the a) one-region and b) two-region waveguide. Three cases of pump wavelength detuning are shown for each.

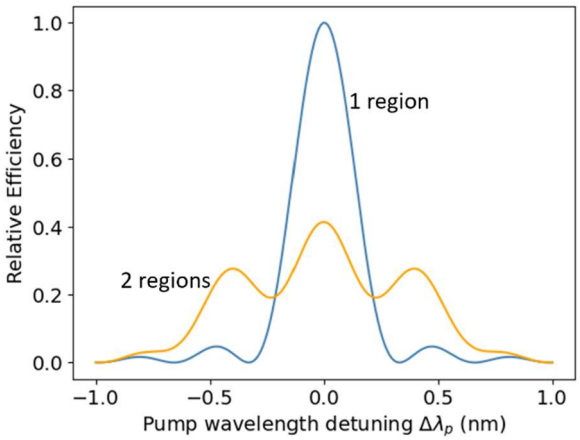


Figure 6. Sensitivity of the one-region (blue curve) and two-region (yellow curve) to detuning of the pump wavelength.

## 6. EXTENTION TO MORE POLING PERIODS

In addition to the two-region waveguide approach, we tried several other approaches to varying the poling periods across the waveguide. These additional attempts involve choosing some functional form for the phase-matching temperature of different regions along length of the waveguide. For example, we look at altering the phase-matching temperature of each region according to a Gaussian function, such that the first and last regions are phase matched to the lowest temperatures and the middle regions to the highest temperatures. We also looked at linearly increasing the phase-matching temperature, as well as altering it according to a tangent curve.

### 6.1 Linearly increasing the phase-matching temperature

Figure 7 shows the relative efficiency of a ten-region waveguide with phase-matching temperatures that vary linearly, as a tangent and Gaussian functions. By first choosing the total number of regions, then iteratively altering the shape of the functional form the phase-matching temperatures followed (lowest and highest phase-matching temperature, width of Gaussian, range of tangent, etc.), we were able to find the smoothest and highest relative efficiency over a

range of ambient temperatures. The best method for increasing the temperature bandwidth was, as is shown in Fig. 7, linearly increasing the phase-matching temperature from 8 °C and 34.5 °C over the length of the waveguide.

The relative efficiency of each curve far outperforms the factor of $1/(10^2) = 0.01$ (red line) that modulates the sum of the different efficiency curves. This is due to the coherent addition of many overlapping regions – the $1/N^2$ scaling would only be expected strictly for the case where there the efficiency curves are separated so far that they do not overlap. It is by careful choice, through optimization, that the result of so many overlapping efficiency curves adds more coherently than incoherently. The regions' efficiency curves add more coherently over the different regions for the case of linearly increasing phase-matching temperature, so it has the broadest temperature bandwidth. For this method, the full width at half maximum temperature bandwidth is about 40 °C, which is over a twofold improvement over our findings for an optimal two-region waveguide and approximately an eightfold improvement over a traditional uniformly poled waveguide.

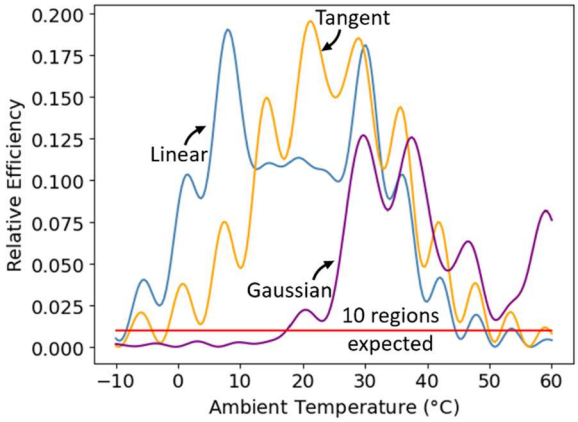


Figure 7. Changing the poling period's phase matching temperature according to a positively sloped linear (blue), tangent (yellow), and Gaussian (purple) functions, with ten regions of different poling period along the length of the waveguide. These are the most coherent choices. The red line is the minimum expected efficiency of ten regions given no coherent addition of efficiencies.

### 6.2 Problems with using more than two regions

The difficulty with realizing the ten-region waveguide is in its fabrication. Ten steps between phase-matching temperatures of 8 °C and 34.5 °C corresponds to changes in poling period on the order of nanometers per region, challenging the precision of current fabrication techniques. Therefore, it is more practical to try replicating these results experimentally for a waveguide with few regions that have larger poling period differences between them. However, as is shown in Fig. 7, there are diminishing returns on each additional region, with an increase in fabrication difficulties.

Even in the simpler case of fewer regions in a waveguide, it is likely that the efficiency vs. temperature curve will still be plagued by interference caused by inconsistencies in the fabrication process. The introduction of differential heating, as discussed in Section 4, can help correct these inconsistencies, but correcting multiple regions with different temperatures is almost certainly an unreasonable goal. Therefore, although we theoretically could make the waveguide's operating temperature bandwidth much wider, the two-region waveguide with corrective differential heating approach may be the best overall solution.

### 6.3 Diminishing returns

The most dramatic improvement in the temperature bandwidth comes from the addition of a second region of a different poling period. Figure 8 shows the relative efficiency curves for 2, 10, and 100 regions of linearly increasing phase-matching temperature. This further reinforces our claim that the most practical solution is to use the two-region waveguide approach, alongside the fabrication difficulties.

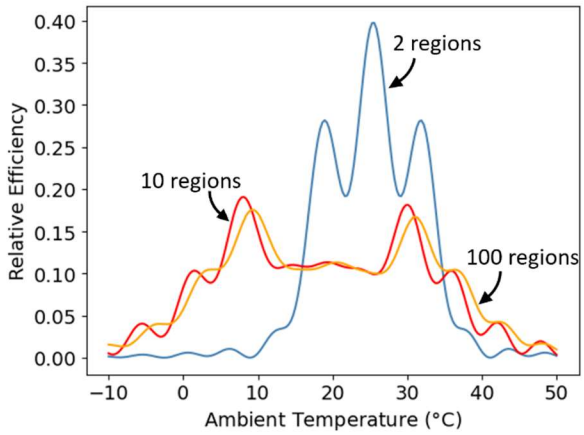


Figure 8. The diminishing returns in 2 (blue), 10 (red), and 100 (orange) linearly increasing phase-matched temperature regions.

### 6.4 Extension to a longer crystal

For some systems, it may be more desirable to have a flatter response to changes in temperature, such that the SPDC efficiency is approximately constant throughout the temperatures considered. For our technique, this is simply not possible – the three-peak efficiency curve from the two-region waveguide is as flat a response we can achieve given the two interacting efficiency curves from the two regions.

A longer waveguide sharpens the efficiency peaks over temperature and lowers maximum efficiencies due to more destructive interference over the longer interaction length $L$. However, the additional length can compensate for lower efficiencies caused by greater separation between the efficiency curves for different poling periods. As a reminder, the intensity of photon pairs generated scales as $L^2$. Therefore, if a flat efficiency response to changes in temperature is required for a given application, we recommend the use of a longer waveguide.

Figure 9 shows the relative efficiency curves of waveguides with 3, 10, 50, and 100 regions. Each has a linearly increasing phase-matching temperature from 15 to 35 °C. These results clearly illustrate how the region-to-region interactions contribute to the overall efficiency curve of the waveguide. The response of the three-region waveguide is clearly three separate efficiency curves, only interacting on the far fringes. The response of the one-hundred-region waveguide is much flatter, with a very broad (almost 50 °C) temperature bandwidth. The difficulties listed in subsection 6.2 will still plague this waveguide though, so unless there is a great deal of progress in fabrication techniques, this method is generally inadvisable.

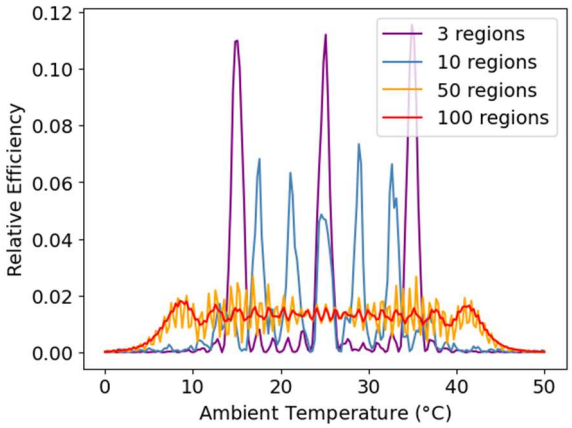


Figure 9. The temperature dependent relative efficiency for 3 (purple), 10 (blue), 50 (yellow), and 100 (red) regions of poling periods with linearly increasing phase-matching temperature.

### 6.5 Temperature Gradient

Another option available to more reliably alter the poling period across the length of the waveguide would be to introduce a temperature gradient to a uniformly poled waveguide. This method would be similar to a constant linear chirp, with the addition of changes due to the temperature-sensitive refractive indices. Simulations of this setup are difficult – there is finite temperature diffusion across the waveguide. Therefore, to see how the waveguide behaves under a temperature gradient, one would have to solve the heat diffusion equation in the volume of the crystal for a given heater setup. The results would then be used alongside the thermal expansion/contraction, as well as the refractive indices' temperature-dependent response to get an accurate picture of the efficiency curve over ambient temperature range. We recommend this as a possible solution to producing a flatter efficiency response while avoiding engineering difficulties discussed in subsection 6.2.

## 7. OTHER PHASE MATCHING CONFIGURATIONS

The phase-matching configuration we used in our simulations was the Type 0 eee (extraordinarily polarized pump, signal, and idler photons, respectively). This choice is both practical and customary – the eee interaction in lithium niobate has a particularly large effective second-order nonlinear susceptibility $d_{\text{eff}}$, which is equal to half the sum of nonzero elements of the second-order nonlinear susceptibility $\chi^{(2)}$ after projecting the three interacting photons onto their corresponding polarization state. Specifically, $d_{\text{eff}}$ for the eee interaction in lithium niobate is about a factor of ten greater than that of the Type 0 ooo interaction, and about a factor of five greater than that of the Type II oeo interaction. The down-converted photon pair production rate scales as $d_{\text{eff}}^2$, so the Type 0 eee produces 100 times more photon pairs than Type 0 ooo for a given pump power. The relative efficiency curves over temperature for these three phase-matching configurations are shown in Fig. 10.

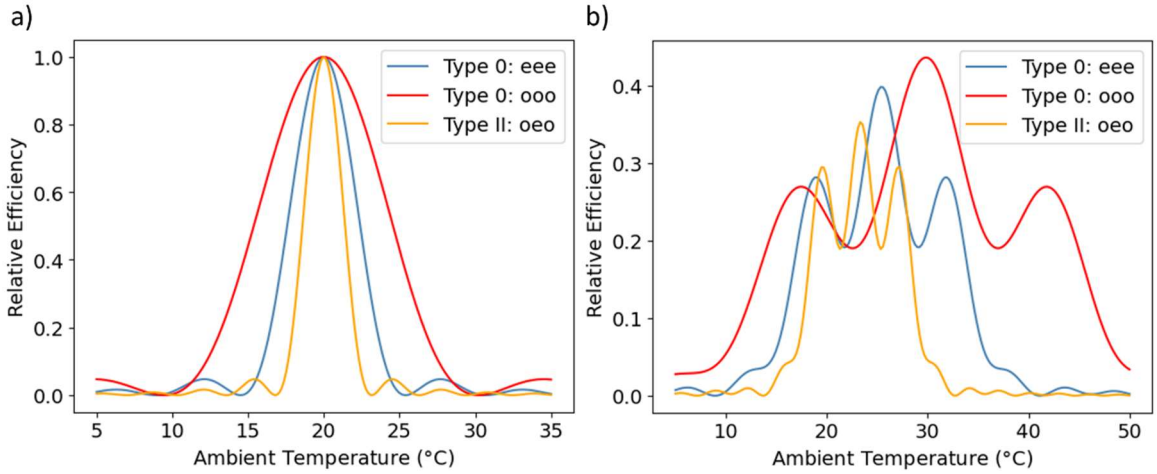


Figure 10. The relative efficiency of down conversion for a) one-region and a b) two-region waveguide. The curves represent different phase-matching configurations: Type 0 eee (blue), Type 0 ooo (red), and Type II oeo (yellow).

It is clear from the efficiency curves in Fig. 10 that the ooo interaction has nearly twice the temperature bandwidth of the eee interaction (and oeo is narrower) for both the one- and two-region waveguide. This result is due to the ordinary refractive index having a smaller temperature sensitivity, as seen in Fig. 1. Therefore, if using 100 times the pump laser power for the same number of down converted photons is not an issue, the ooo interaction is something that should be considered for its greatly reduced temperature sensitivity.

## 8. CONCLUSIONS

Periodically-poled SPDC sources are naturally suited for producing time-frequency entangled photonic states, but traditional one-region waveguides are typically quite sensitive to temperature fluctuations in their environment often requiring precise temperature control. Additionally, setups that rely on degenerate photon pairs without strict down-converted photon wavelength requirements need to also have careful control over laser temperature because the pump wavelength's changes with temperature may push the efficient operating temperature range out of reach for current ambient conditions. We ease both of these difficulties here by shifting from a one-region to a two-region design of

periodically-poled waveguides, minimizing the amount of thermal control needed for efficient down conversion. Furthermore, we show that manufacturing error in the poling periods can be remediated by differential heating of the two regions, which is less costly in terms of SWaP than heating the entire crystal. We extend our technique to more poling periods and show that this approach has diminishing returns due to increased fabrication difficulties. We also show that different phase-matching configurations have varying temperature bandwidth, and we explain that any benefit from choosing Type 0 ooo over Type 0 eee must be weighed against a smaller magnitude of effective nonlinear susceptibility.

The computer code used to generate these plots is written in Python and can be made available upon request.

## ACKNOWLEDGEMENTS

We gratefully acknowledge the financial support of the National Aeronautics and Space Administration (NASA) STTR Phase I: Compact temperature tolerant quantum entangled light source, SRICO, Inc., Subcontract No. 22053OSUD, and scientific discussions with Vincent Stenger, Andrea Pollick, and Sri Sriram.

## REFERENCES

[1] N. Gisin and R. Thew, "Quantum communication," Nature Photon. **1**, 165 (2007).
[2] M. M. Fejer, G. A. Magel, D. H. Jundt, and R. L. Beyer, 'Quasi-phase-matched second harmonic generation: tuning and tolerances,' IEEE J. Quantum Electron. **28**, 2631 (1992).
[3] G. Chen, H.-L. Lin, and A. J. Danner, 'Highly efficient thermal tuning interferometer in lithium niobate thin file using air bridge,' IEEE Photonics J. **13**, 6600409 (2021).
[4] A. Tehranchi and R. Kashyap, 'Engineered gratings for flat broadening of second-harmonic phase-matching bandwidth in MgO-doped lithium niobate waveguides,' Opt. Express **16**, 18970 (2008).
[5] N. Balaji, T. S. Meetei, M. M. Ali, S. Boomadevi, M. Senthilkumar, and K. Pandiyan, 'Generation of nearly flattop ultrabroadband response in a QPM device using phase shifter. J. Lightwave Tech. **37**, 845 (2019).
[6] Bartnick *et al*., 'Cryogenic Second-Harmonic Generation in Periodically Poled Lithium Niobate Waveguides,' Phys. Rev. Appl. **15**, 024028 (2021).
[7] https://www.bostonpiezooptics.com/lithium-niobate
[8] X. Wu, L. Zhang, Z. Hao, R. Zhang, R. Ma, F. Bo, G. Zhang, and J. Xu, 'Broadband second harmonic generation in step-chirped periodically poled lithium niobate waveguides,' Opt. Lett. **47**, 1574 (2022).